Published in final edited form as:
Biochim Biophys Acta. 2009 December ; 1794(12): 1831–1837. doi:10.1016/j.bbapap.2009.08.022.

The Reaction Mechanism of Phenylethanolamine *N*-Methyltransferase: A Density Functional Theory Study

Polina Georgieva[1], **Qian Wu**[2], **Michael J. McLeish**[2,3,*], and **Fahmi Himo**[1,*]

[1]Department of Theoretical Chemistry, School of Biotechnology, Royal Institute of Technology, SE-106 91 Stockholm – Sweden

[2]Department of Medicinal Chemistry, University of Michigan, Ann Arbor, MI 48109 USA

[3]Department of Chemistry and Chemical Biology, Indiana University-Purdue University Indianapolis, Indianapolis IN 46202 USA

Summary

Hybrid density functional theory methods were used to investigate the reaction mechanism of human phenylethanolamine *N*-methyltransferase (hPNMT). This enzyme catalyzes the *S*-adenosyl-L-methionine-dependent conversion of norepinephrine to epinephrine, which constitutes the terminal step in the catecholamine biosynthesis. Several models of the active site were constructed based on the X-ray structure. Geometries of the stationary points along the reaction path were optimized and the reaction barrier and energy were calculated and compared to the experimental values. The calculations demonstrate that the reaction takes place via an S_N2 mechanism with methyl transfer being rate-limiting, a suggestion supported by mutagenesis studies. Optimal agreement with experimental data is reached using a model in which both active site glutamates are protonated. Overall, the mechanism of hPNMT is more similar to those of catechol *O*-methyltransferase and glycine *N*-methyltransferase than to that of guanidinoacetate *N*-methyltransferase in which methyl transfer is coupled to proton transfer.

1. Introduction

Phenylethanolamine *N*-methyltransferase (PNMT; EC 2.1.1.28) catalyzes the terminal step in catecholamine biosynthesis, i.e., the *S*-adenosyl-L-methionine (AdoMet)-dependent conversion of norepinephrine to epinephrine (adrenaline, Scheme 1) [1,2].

PNMT is found in high levels in the adrenal medulla [2] where epinephrine is secreted as a hormone, particularly during periods of stress. In addition, epinephrine (Epi) makes up 5–10% of the total catecholamine content of the brain, but its function within the central nervous system (CNS) is not well understood [3]. In the past CNS epinephrine has been implicated in a wide range of activities including central control of blood pressure and respiration [4,5], the secretion of hormones from the pituitary [6], the control of exercise tolerance [7] and the activation of

*Address correspondence to these authors: Fahmi Himo Ph.D., Department of Organic Chemistry, Arrhenius Laboratory, Stockholm University, SE-10691 Stockholm - Sweden, Tel: +46 8 161094, himo@organ.su.se, Michael J. McLeish Ph.D., Department of Chemistry & Chemical Biology, Indiana University-Purdue University Indianapolis, 402 N. Blackford St, Indianapolis IN 46202 USA, Tel: +1 317 274 6889, mcleish@iupui.edu.

the α_1-adrenoceptor [8]. It may even be responsible for some of the neurodegeneration found in Alzheimer's disease [9]. As a consequence there has been a lot of effort expended in obtaining inhibitors of human PNMT (hPNMT) that would help delineate of the role of central Epi, and that may ultimately be of pharmaceutical benefit [10–12]

Recently, a number of X-ray structures have been obtained which show hPNMT in complex with a variety of substrates and inhibitors [13–15]. In each case the complex also contained either AdoMet or the product, *S*-adenosyl-L-homocysteine (AdoHcy). Comparison of the structures indicated that in each case the positions of the ligands were virtually identical, allowing us to construct a composite structure of the hPNMT active site. This structure, which includes the two substrates, *p*-octopamine (representing Epi) and AdoMet, as well as several residues believed to be catalytically important, is shown in Figure 1.

The aromatic ring of the PNMT substrates is sandwiched between Phe182 (not shown) and Asn39 [13]. The phenolic hydroxyl of octopamine helps orient the substrate by interacting with Lys57 via a water molecule. The β-hydroxyl is within hydrogen bonding distance of Glu219 and also has strong water-mediated interactions with Asn39 and Asp267 [13,14]. Mutagenesis studies have shown that the latter interaction is particularly important in positioning the ethanolamine sidechain for catalysis [15]. The sidechain itself is in an extended conformation so that the C—N distance in an AdoMet-octopamine model structure (Figure 1) is ca. 3.7 Å [15], well within that expected for methyl transfer (3.0–4.0 Å) [16]. Overall, the sidechain is positioned for nucleophilic attack by the substrate on the activated methyl group of AdoMet.

Small molecule methyltransferases are thought to catalyze direct transfer of the methyl group from AdoMet to the substrate via an S_N2 mechanism [17]. In order for nucleophilic attack to take place, the amine of the sidechain must be deprotonated. This may occur in two ways. In the first, exemplified by glycine *N*-methyltransferase (GNMT), it appears that the substrate binds in a neutral form [18] and that methyl group transfer is rate-limiting [19]. In the second, exemplified by guanidinoacetate *N*-methyltransferase (GAMT), the substrate binds and is subsequently deprotonated by direct interaction with an active site aspartic acid residue [20]. Later, it was shown that methyl transfer was coupled to proton transfer [21]. In PNMT the situation is not so clear cut. In general, hPNMT assays are carried out at pH 8.0 and the amine pK_a of substrates such as noradrenaline, phenylethanolamine and *p*-octopamine is ~8.5 (MJ McLeish, unpublished). Under those assay conditions, the majority of the substrate would be expected to be protonated. Based on the active site shown in Figure 1 it is reasonable to assume that a protonated amine could be deprotonated by either Glu185 or Glu219. Of course, at pH 8.0 a significant proportion of the substrate will not be protonated and, in the absence of any pH-rate data, the possibility that the substrate binds in neutral form cannot be ruled out. It should be also noted that, as detailed in Table 1, mutagenesis studies have provided k_{cat} values for Glu185 and Glu219 variants that are not consistent with deprotonation by either residue being the rate determining step in the hPNMT-catalyzed reaction [15].

In recent years a density functional theory method, B3LYP [22–26], has proved very successful in studying enzyme active sites and reaction mechanisms, including those of the small molecule methyltransferases GNMT [27] and GAMT [21]. The utility of the method has been described in a series of recent reviews [28–31] and it seemed an appropriate tool to extend our investigation of the reaction mechanism of hPNMT [15,32]. Here we describe the design of models of the active site based on the hPNMT X-ray structure. Reaction barriers and energies were calculated and compared to that derived from experimental data. In addition, site-directed mutagenesis was used to examine the relative importance of Glu185 and Glu219 in catalysis.

2. Materials and methods

2.1. Calculations

All calculations presented here were performed using the B3LYP [22–26] density functional method as implemented in Gaussian03 program package [33]. Geometry optimizations were performed using the 6–31G(d,p) basis set. Based on these optimized geometries, single point calculations with the larger basis set 6–311+G(2d,2p) were done to obtain more accurate energies. To estimate solvation effects of that part of the enzyme that is not included in the quantum cluster, single point calculations on the optimized geometries were performed with the conductor–like polarizable continuum model (CPCM) [34,35] at the B3LYP/6–31G(d,p) level with two dielectric constants, ε=4 and ε=80. Hessians were calculated at the B3LYP/6–31G(d,p) level to confirm the nature of the optimized stationary points. The Hessians were also used to calculate zero-point vibrational effects. Since some centers were kept fixed to their X-ray positions in the geometry optimization (see below), a few small imaginary frequencies usually appear, typically on order of $10i$–$20i$ cm^{-1}. These frequencies do not contribute significantly to the zero-point energies and can thus be ignored.

2.2 Preparation and characterization of hPNMT E185A/E219A

The E185A primer was available from a previous study [15]. The double mutant was prepared using Pfu DNA polymerase and the QuikChange site-directed mutagenesis kit (Stratagene), using pET17PNMT-his E219A [32] as the DNA template. The fidelity of the PCR amplification and the presence of both mutations were confirmed by sequencing. The plasmid was then transformed into *E. coli* strain BL21(DE3)pLysS (Novagen) and the enzyme was expressed and purified by affinity followed by size exclusion chromatography. The purified enzyme was assayed under standard assay conditions and the data fit to the equation for a sequential mechanism as described previously [36].

3. Results and discussion

Three models of the PNMT active site were constructed in order to develop deeper understanding of the reaction taking place. The models are of increasing size and are based on the X-ray crystal structure of PNMT in complex with AdoHcy and *p*-octopamine (PDB code 2AN4) [13]. Hydrogen atoms were added manually and AdoHcy was converted to AdoMet by adding a methyl group at the S position. AdoMet was modeled by truncating the cofactor two carbons away on each side of the sulfur center. Based on our previous experience, this model of AdoMet is sufficient to reproduce the properties of the S—C bond, and it has enough flexibility to accommodate structural changes during the reaction [21,27]. In the largest model (Model C, see below) an additional carbon was kept. The truncation points of both AdoMet and the various active site residues were kept fixed during geometry optimization in order to prevent large spatial reorganization of the active site residues and to keep the model geometrically close to the X-ray crystal structure. These fixed centers are indicated by arrows in Figure 2–Figure 5. To recover the solvation of regions of the protein that are not included in the models, a dielectric continuum model was adopted. In this scheme, a cavity is created around the solute and it is surrounded by polarizable dielectric continuum. Two dielectric constants were used, ε=4 and ε= 80. The former is a standard value used in protein modeling, and the latter corresponds to water solution.

3.1 Model A

The smallest conceivable model of the PNMT active site is composed only of truncated models of the AdoMet cofactor and the substrate as shown in Figure 2. The substrate is modeled in the neutral form and the phenyl group is replaced by a hydrogen atom. No other active site residues are included. This model, called Model A, therefore comprises 30 atoms and has a total charge

of +1. The optimized structures of the reactant, transition state (TS), and product state of this model are shown in Figure 2.

Similarly to GNMT [27], in this model the methyl transfer was found to occur through an S_N2 mechanism. At the TS, the critical S−C and C−N distances are 2.36 Å and 2.19 Å, respectively, which are quite similar to the distances found for GNMT (2.38 Å and 2.20 Å) [27]. The TS has an imaginary frequency of $-406i$ cm^{-1}. The barrier for the transfer was calculated to be 16.7 kcal/mol, which upon inclusion of solvation effects remains relatively unchanged at 16.6 kcal/mol (ε=4) and 16.4 kcal/mol (ε=80) (Table 2). The barriers for this very small model agree surprisingly well with the experimentally-measured rate constant of 2.8 min^{-1} (Table 1), which can be converted to a barrier of ca. 19 kcal/mol using classical transition state theory. In addition, the reaction is calculated to be exothermic by 5.7 kcal/mol (13.2 and 15.8 kcal/mol including solvation with ε=4 and ε=80, respectively).

The fact that this small model yields good results compared to experiments indicates that a major part of the elements necessary to describe the reaction are already captured in the model. However, it must be admitted that the good agreement may well be the result a significant degree of error cancellation.

3.2. Model B

A somewhat larger model of the PNMT active site, called Model B, was devised, which consisted of 48 atoms. In addition to the parts used in Model A, this model also includes Glu185 and Glu219 (represented by acetates) and a water molecule (W1), which initially was bridging the substrate and the Glu185 residue (Figure 1). Both glutamate residues were initially modeled in the deprotonated form, and the substrate was modeled as a cation, i.e. in its protonated state. The total charge of the model is thus 0. In the optimization, a proton moved immediately from the amino group of the substrate to Glu185, through the bridging water molecule, which subsequently moved out to bridge the two glutamate groups instead (see Figure 3). Effectively, in this model the substrate is in the neutral form and one of the glutamates, likely Glu185, is protonated. We note that, in the model, the OH group of the Glu185 carboxylate is not in the (slightly) preferred syn-periplanar orientation relative the C=O bond. However, as we are only concerned with relative energies in this study, and the position of the proton is the same in all stationary points of the model (Figure 3), this energy difference cancels and the orientation of the OH group becomes unimportant.

Using this reactant structure, a TS for the methyl transfer was located (structure B in Figure 3). The TS is characterized by an imaginary frequency of $-359i$ cm^{-1}, and the S−C and C−N distances are calculated to be 2.22 Å and 2.40 Å, respectively. This shows that the TS in this model occurs earlier than in Model A (cf. Figure 2), which is also evident from the activation barrier. Model B has a calculated barrier of 6.0 kcal/mol without solvation effects, which increases to 11.8 and 13.7 kcal/mol, using ε=4 and ε=80, respectively. These values are significantly lower than those found for Model A. It is easy to rationalize this result if one recognizes that in the reaction a methyl cation is transferred to the substrate. In the case of Model B an anionic glutamate is present that can stabilize the product better than the substrate, lowering thus the barrier for the reaction. This fact is even more evident from the calculated exothermicity of the reaction. The product complex (structure C in Figure 3) has an energy that lies at −48.3 kcal/mol compared to the reactant (−28.5 and −21.8 kcal/mol when ε=4 and ε=80 are used, respectively).

Assuming Glu219 remains in the deprotonated form, it is now possible for it to pick up a proton from the methylated product molecule. We have optimized the structure in which a proton from the product nitrogen has transferred to Glu219 (structure D in Figure 3). This structure has a

very similar energy compared to the other product structure; −47.9, −27.7 and −20.9 kcal/mol, without solvation, and with ε=4 and ε=80, respectively.

3.3. Model C

The fact that the smaller Model A agrees better than Model B with the experimental rate indicates that either something is missing in Model B or that the model is unbalanced. We have therefore created a much larger model (Model C), consisting of 93 atoms, which is shown in Figure 4. In addition to the parts included in Model B, this model contains parts of the amino acids Asp267, Arg44, and Asn39. A second water molecule (W2, Figure 1) observed in the crystal structure is also included. In addition, to grant even more flexibility to the model, a complete (i.e., not truncated) substrate was used and one more carbon was kept in the AdoMet. Given that the vast majority of kinetic and mutagenesis studies with hPNMT are carried out with phenylethanolamine [15,32,36,37], for comparative purposes it seemed logical to use this as the substrate in the larger model. Using phenylethanolamine has an additional advantage in that it oviates the need to include W3 and Lys57 in the model. The total charge of model C is 0 and, as in the case of Model B, the substrate was initially modeled in the protonated form and the two glutamates (Glu185 and Glu219) were anionic. Also here, during the geometry optimization of the reactant a proton was transferred spontaneously from the amino group of the substrate to the Glu185 residue through a water bridge (Figure 4).

The TS for the methyl transfer in Model C was optimized and is also displayed in Figure 4. This TS is characterized by an imaginary frequency of $-351i\ cm^{-1}$, and S−C and C−N distances of 11 2.11 Å and 2.35 Å, respectively. We find that the TS now is even earlier than in Model B. The calculated reaction barrier is 4.8 kcal/mol, which increases to 8.8 and 9.9 kcal/mol when solvation effects using ε=4 and ε=80, respectively, are accounted for (Table 1). We find that simultaneously with the methyl transfer, a proton is transferred from the substrate to Glu219. The reaction is exothermic by 47.9 kcal/mol, which, as in the case of Model B, is considerably decreased to −29.5 and −28.3 kcal/mol, when ε=4 and ε=80 are used, respectively. Based on these results it would appear that the presence of the two carboxylates close to the substrate makes the barrier for the methyl transfer much lower than, and consequently inconsistent with, the barrier estimated from the experimental rate constant (ca. 19 kcal/mol).

Since inclusion of the negatively-charged Glu185 and Glu219 consistently lowers the energy barrier in both Models B and C, we explored the possibility of having one of them protonated. In the first instance, a proton was added to Glu219. The model, called Model C(H^+), now has a total charge of +1. The optimized geometries of the reactant, TS, and product species are shown in Figure 5. Again, although the substrate was modeled in its protonated state, a proton spontaneously moved to Glu185 during the geometry optimization. The reaction barrier was calculated to be 13.6 kcal/mol (15.8 and 16.4 kcal/mol including ε=4 and ε=80, respectively). These values are now in much better agreement with the experimental rate compared to the Models B and C, in which only one of the glutamates is protonated.

Overall these results strongly suggest that either the two active site glutamates are both in the protonated form prior to the binding of a neutral substrate, or that one of them is protonated and the other receives a proton from a cationic substrate. Given that typical phenylethanolamine pK_a values are around 8.5, it is unlikely that, under the standard assay conditions of pH 8.0, the substrate binds in neutral form. Therefore the latter explanation would be the more likely. This would require that at least one of the glutamates has a pK_a value above pH 8–8.5.

Recently a method was developed which permitted the rapid prediction of pK_a values for ionizable residues in proteins [38]. The method, PROPKA, has now been extended to include the effects of ligands on these protein pK_a values [39]. PROPKA uses the data contained in PDB files which has enabled us to predict the pK_a of both Glu185 and Glu219 in structures

with either amine substrates or THIQ-based inhibitors bound in the active site. The overall results show that Glu185 is expected to have a pK_a around 6 whereas Glu219 will have a pK_a around 9. This is consistent with our results with Model C(H^+) which requires that one of the glutamates is protonated and the other receives a proton from a cationic substrate.

3.4. Mutagenesis of Glu185 and Glu219

Previous studies [15,32] have reported that the k_{cat} values for the alanine variants of Glu185 and Glu219 show only a 16-fold and a 2-fold decrease over the wild type k_{cat} value, respectively (Table 1). Further, the E219Q variant shows wild-type activity and, overall, these results are inconsistent with deprotonation of the substrate being rate limiting. Only the E185Q variant shows a significant (300-fold) decrease in k_{cat} value and even that has been attributed to alterations in the geometry of the active site (N. Drinkwater and J. L. Martin, personal communication).

The computational model suggests that it is necessary for one of the glutamates to be protonated (i.e., in neutral form) and that the other able to accept a proton from the substrate. That said, it is not clear from the model which residue needs to be deprotonated, and the mutagenesis data suggests that either residue may be acceptable. Therefore, to take this issue a little further, a hPNMT variant was prepared in which both glutamates had been replaced with alanine. The expression and purification of the E185A/E219A variant was accomplished using routine procedures. The enzyme was stable and exhibited normal kinetic behavior. The K_m values for both substrates were similar to the wild-type value, while the k_{cat} value decreased only 10-fold (Table 1). Taken together the results suggest that neither residue contributes to a rate-limiting step in the mechanism.

3.5 Comparison with other small molecule methyltransferases

Catechol *O*-methyltransferase (COMT), GNMT and GAMT are three of the best characterized small molecule methyltransferases. The mechanism of COMT, in particular, has undergone considerable study including the early identification of an S_N2 mechanism [19,40] and the use of kinetic isotope effects to show that methyl transfer is rate limiting [19]. Recent computational studies confirm that observation [41] and suggest that the prime role of the enzyme in catalysis is to arrange the substrates in the ground state so that their conformation resembles that of the transition state [42,43]. Given its pK_a the catechol would be expected to bind in a neutral form. Consequently, a second role for the enzyme is to provide a basic group to remove a proton from the catechol which is necessary for the reaction to proceed [41]. Formation of the catecholate also has the effect of orienting the cationic AdoMet so that the probability of methyl group transfer is increased [43].

A similar situation obtains in GNMT where the substrate is thought to bind with a neutral amino group and is held tightly in place by 7 hydrogen bonds which have the dual effect of holding the substrate firmly in place and orienting the lone pair of the nitrogen towards the C of AdoMet [18]. Again, calculations show that that methyl transfer occurs in a single step and confirm mutagenesis results indicating that hydrogen bonds to the amino group of the substrate lower the reaction barrier [27].

By contrast, the reaction mechanism of GAMT showed some surprising differences. Superficially, the active site of GAMT looks most like that of PNMT in that there is a carboxylate (Asp134) positioned to remove a proton from the amine of the substrate, in this instance the N_E of guanidinoacetate [20]. This residue could correspond to either Glu185 or Glu219 in hPNMT (Figure 1). As with the hPNMT E185Q variant, the k_{cat} of the amide (D134N) mutant was reduced by two orders of magnitude but, unlike E185A or E219A (Table 1), the D134A variant was inactive [20]. A second difference was that density functional

analysis showed that methyl transfer from AdoMet was coupled to the movement of the proton from guanidinoacetate to Asp134 [21]. Presumably, it is this coupling that is reflected in the lack of activity of the GAMT D134A variant.

The previous mutagenesis results for hPNMT indicate that, in spite of the presence of two carboxylates adjacent to the amine of the substrate, it is likely that hPNMT catalyzes methyl transfer in a manner more akin to COMT and GNMT than to GAMT. Here the calculations confirm that prediction and show that the rate-limiting methyl transfer step is not coupled to proton movement. Rather, proton transfer to Glu185 was seen to occur spontaneously upon substrate binding.

4. Conclusions

In the present study, three quantum chemical active site models have been employed to investigate the methyl transfer reaction mechanism in hPNMT. All models confirm that the methyl transfer reaction takes place via an S_N2 mechanism. The calculated barriers, however, vary considerably among the models. With the smallest model (Model A), which only consists of truncated models of AdoMet and the substrate, the calculated energy barrier was found to be in relatively good agreement with that calculated from the experimental rate constant. However, when additional groups of the active site were added, including the important Glu185 and Glu219 residues, the barrier dropped and the models (Models B and C) yielded worse agreement with the experimental barrier. Further analysis showed that the disagreement arose because the carboxylates of Glu185 and Glu219 were modeled in their anionic form. Much better agreement with the experimental barrier is reached with Model C(H^+) in which both glutamates are protonated and the substrate binds in neutral form. Alternatively, this could occur if one of the glutamates is protonated initially while the other receives a proton from a protonated substrate. Consistent with the latter proposal are the PROPKA predictions that the pK_a of Glu185 is around 6 whereas that of Glu219 is around 9, as well as mutagenesis results indicating that proton transfer is not rate-limiting. Overall, the mechanism of hPNMT is more similar to those of COMT and GNMT than to that of GAMT.

Acknowledgments

FH gratefully acknowledges financial help from: The Swedish Research Council, The Wenner-Gren Foundations, The Carl Trygger Foundation, and The Magn Bergvall Foundation. MJM acknowledges the support of a grant from the National Institutes of Health (RO1 HL34193).

REFERENCES

1. Kirshner N, Goodall M. The formation of adrenaline from noradrenaline. Biochim. Biophys. Acta 1957;24:658–659. [PubMed: 13436503]
2. Axelrod J. Purification and properties of phenylethanolamine *N*-methyltransferase. J. Biol. Chem 1962;237:1657–1660. [PubMed: 13863458]
3. Fuller, RW. Overview and concluding remarks. In: Stolk, JM.; U'Prichard, DC.; Fuxe, K., editors. Epinephrine in the Central Nervous System. New York: Oxford University Press; 1988. p. 366-369.
4. Hokfelt T, Fuxe K, Goldstein M, Johannson O. Immunohistochemical evidence for the existence of adrenaline neurons in the rat brain. Brain Res 1974;66:235–251.
5. Black J, Waeber B, Bresnahan MR, Gavras I, Gavras H. Blood pressure response to central and/or peripheral inhibition of phenylethanolamine *N*-methyltransferase in normotensive and hypertensive rats. Circ. Res 1981;49:518–524. [PubMed: 7249286]
6. Crowley WR, Terry LC, Johnson MD. Evidence for the involvement of central epinephrine systems in the regulation of luteinizing hormone, prolactin, and growth hormone release in female rats. Endocrinology 1982;110:1102–1107. [PubMed: 7037366]

7. Trudeau F, Brisson GR, Peronnet F. PNMT inhibition decreases exercise performance in the rat. Physiol. Behav 1992;52:389–392. [PubMed: 1523268]
8. Stone EA, Grunewald GL, Lin Y, Ahsan R, Rosengarten H, Kramer HK, Quartermain D. Role of epinephrine stimulation of CNS α_1-adrenoceptors in motor activity in mice. Synapse 2003;49:67–76. [PubMed: 12710017]
9. Burke WJ, Galvin NJ, Chung HD, Stoff SA, Gillespie KN, Cataldo AM, Nixon RA. Degenerative changes in epinephrine tonic vasomotor neurons in Alzheimer's disease. Brain Res 1994;661:35–42. [PubMed: 7834382]
10. Kaiser C, Pendleton RG. Specific inhibition of adrenal epinephrine biosynthesis as a potential source of therapeutic agents. Intra-Science Chem. Rept 1974;8:43–55.
11. Bondinell WE, Chapin FW, Frazee JS, Girard GR, Holden KG, Kaiser C, Maryanoff C, Perchonock CD, Gessner GW, Hieble JP, et al. Inhibitors of phenylethanolamine *N*-methyltransferase and epinephrine biosynthesis: a potential source of new drugs. Drug. Metab. Rev 1983;14:709–721. [PubMed: 6352222]
12. Grunewald GL, Romero FA, Criscione KR. Nanomolar inhibitors of CNS epinephrine biosynthesis: (R)-(+)-3-fluoromethyl-7-(N-substituted aminosulfonyl)-1,2,3,4-tetrahydroisoquinolines as potent and highly selective inhibitors of phenylethanolamine N-methyltransferase. J. Med. Chem 2005;48:1806–1812. [PubMed: 15771426]
13. Martin JL, Begun J, McLeish MJ, Caine JM, Grunewald GL. Getting the adrenaline going: crystal structure of the adrenaline-synthesizing enzyme PNMT. Structure 2001;9:977–985. [PubMed: 11591352]
14. McMillan FM, Archbold J, McLeish MJ, Caine JM, Criscione KR, Grunewald GL, Martin JL. Molecular recognition of sub-micromolar inhibitors by the epinephrine-synthesizing enzyme phenylethanolamine *N*-methyltransferase. J. Med. Chem 2004;47:37–44. [PubMed: 14695818]
15. Gee CL, Tyndall JDA, Grunewald GL, Wu Q, McLeish MJ, Martin JL. Mode of binding of methyl acceptor substrates to the adrenaline-synthesizing enzyme phenylethanolamine *N*-methyltransferase: implications for catalysis. Biochemistry 2005;44:16875–16885. [PubMed: 16363801]
16. Svetlitchnaia T, Svetlitchnyi V, Meyer O, Dobbek H. Structural insights into methyltransfer reactions of a corrinoid iron-sulfur protein involved in acetyl-CoA synthesis. Proc. Natl. Acad. Sc.i U.S.A 2006;103:14331–14336.
17. Schubert HL, Blumenthal RM, Cheng X. Many paths to methyltransfer: a chronicle of convergence. Trends Biochem. Sci 2003;28:329–335. [PubMed: 12826405]
18. Takata Y, Huang Y, Komoto J, Yamada T, Konishi K, Ogawa H, Gomi T, Fujioka M, Takusagawa F. Catalytic mechanism of glycine *N*-methyltransferase. Biochemistry 2003;42:8394–8402. [PubMed: 12859184]
19. Hegazi MF, Borchard RT, Schowen RL. S_N2-like transition state for methyl transfer catalyzed by catechol-*O*-methyl-transferase. J. Am. Chem. Soc 1976;98:3048–3049. [PubMed: 1262638]
20. Komoto J, Yamada T, Takata Y, Konishi K, Ogawa H, Gomi T, Fujioka M, Takusagawa F. Catalytic mechanism of guanidinoacetate methyltransferase: crystal structures of guanidinoacetate methyltransferase ternary complexes. Biochemistry 2004;43:14385–14394. [PubMed: 15533043]
21. Velichkova P, Himo F. Theoretical study of the methyl transfer in guanidinoacetate methyltransferase. J. Phys. Chem. B 2006;110:16–19. [PubMed: 16471489]
22. Becke AD. Density-functional exchange-energy approximation with correct asymptotic-behavior. Phys. Rev. A 1988;38:3098–3100. [PubMed: 9900728]
23. Becke AD. Density-functional thermochemistry 1. The effect of the exchange-only gradient correction. J. Chem. Phys 1992;96:2155–2160.
24. Becke AD. Density-functional thermochemistry 2. The effect of the Perdew-Wang generalized-gradient correlation correction. J. Chem. Phys 1992;97:9173–9177.
25. Becke AD. Density-functional thermochemistry 3. The role of exact exchange. J. Chem. Phys 1993;98:5648–5652.
26. Stephens PJ, Devlin FJ, Chabalowski CF, Frisch MJ. Ab-initio calculation of vibrational absorption and circular-dichroism spectra using density-functional force-fields. J. Phys. Chem 1994;98:11623–11627.

27. Velichkova P, Himo F. Methyl transfer in glycine *N*-methyltransferase. A theoretical study. J. Phys. Chem. B 2005;109:8216–8219. [PubMed: 16851960]
28. Noodleman L, Lovell T, Han W-G, Li J, Himo F. Quantum chemical studies of Intermediates and reaction pathways in selected enzymes and catalytic synthetic systems. Chem. Rev 2004;104:459–508. [PubMed: 14871132]
29. Himo F. Quantum chemical modeling of enzyme active sites and reaction mechanisms. Theor. Chem. Acc 2006;116:232–240.
30. Siegbahn PEM, Borowski T. Modeling enzymatic reactions involving transition metals. Acc. Chem. Res 2006;39:729–738. [PubMed: 17042473]
31. Ramos MJ, Fernandes PA. Computational enzymatic catalysis. Acc. Chem. Res 2008;41:689–698.
32. Wu Q, Gee CL, Lin F, Tyndall JD, Martin JL, Grunewald GL, McLeish MJ. Structural, mutagenic and kinetic analysis of the binding of substrates and inhibitors of human phenylethanolamine *N*-methyltransferase. J. Med. Chem 2005;48:7243–7252. [PubMed: 16279783]
33. Frisch, MJ.; Trucks, GW.; Schlegel, HB.; Scuseria, GE.; Robb, MA.; Cheeseman, JR.; Montgomery, J.; Vreven, JAT.; Kudin, KN.; Burant, JC.; Millam, JM.; Iyengar, SS.; Tomasi, J.; Barone, V.; Mennucci, B.; Cossi, M.; Scalmani, G.; Rega, N.; Petersson, GA.; Nakatsuji, H.; Hada, M.; Ehara, M.; Toyota, K.; Fukuda, R.; Hasegawa, J.; Ishida, M.; Nakajima, T.; Honda, Y.; Kitao, O.; Nakai, H.; Klene, M.; Li, X.; Knox, JE.; Hratchian, HP.; Cross, JB.; Bakken, V.; Adamo, C.; Jaramillo, J.; Gomperts, R.; Stratmann, RE.; Yazyev, O.; Austin, AJ.; Cammi, R.; Pomelli, C.; Ochterski, JW.; Ayala, PY.; Morokuma, K.; Voth, GA.; Salvador, P.; Dannenberg, JJ.; Zakrzewski, VG.; Dapprich, S.; Daniels, AD.; Strain, MC.; Farkas, O.; Malick, DK.; Rabuck, AD.; Raghavachari, K.; Foresman, JB.; Ortiz, JV.; Cui, Q.; Baboul, AG.; Clifford, S.; Cioslowski, J.; Stefanov, BB.; Liu, G.; Liashenko, A.; Piskorz, P.; Komaromi, I.; Martin, RL.; Fox, DJ.; Keith, T.; Al-Laham, MA.; Peng, CY.; Nanayakkara, A.; Challacombe, M.; Gill, PMW.; Johnson, B.; Chen, W.; Wong, MW.; Gonzalez, C.; Pople, JA. *Gaussian 03* (Revision D.01). Wallingford CT: Gaussian Inc; 2004.
34. Barone V, Cossi M. Quantum calculation of molecular energies and energy gradients in solution by a conductor solvent model. J. Phys. Chem. A 1998;102:1995–2001.
35. Cossi M, Rega N, Scalmani G, Barone V. Energies, structures, and electronic properties of molecules in solution with the C-PCM solvation model. J. Comp. Chem 2003;24:669–681. [PubMed: 12666158]
36. Gee CL, Nourse A, Hsin AY, Wu Q, Tyndall JD, Grunewald GL, Michael MJ, McLeish J, Martin JL. Disulfide-linked dimers of human adrenaline synthesizing enzyme PNMT are catalytically active. Biochim. Biophys. Acta 2005;1750:82–92. [PubMed: 15893506]
37. Gee CL, Drinkwater N, Tyndall JD, Grunewald GL, Wu Q, McLeish MJ, Martin JL. Enzyme adaptation to inhibitor binding: a cryptic binding site in phenylethanolamine *N*-methyltransferase. J. Med. Chem 2007;50:4845–4853. [PubMed: 17845018]
38. Li H, Robertson AD, Jensen JH. Very fast empirical prediction and rationalization of protein pKa values. Prot. Struct. Funct. Bioinf 2005;61:704–721.
39. Bas DC, Rogers DM, Jensen JH. Very fast prediction and rationalization of pK_a values for protein-ligand complexes. Prot. Struct. Funct. Bioinf 2008;73:765–783.
40. Woodard RW, Tsai MD, Floss HG, Crooks PA, Coward JK. Stereochemical course of the transmethylation catalyzed by catechol *O*-methyltransferase. J. Biol. Chem 1980;255:9124–9127. [PubMed: 6997310]
41. Zheng YJ, Bruice TC. A theoretical examination of the factors controlling the catalytic efficiency of a transmethylation enzyme: Catechol *O*-methyltransferase. J. Am. Chem. Soc 1997;119:8137–8145.
42. Kahn K, Bruice TC. Transition-state and ground-state structures and their interaction with the active-site residues in catechol *O*-methyltransferase. J. Am. Chem. Soc 2000;122:46–51.
43. Lau EY, Bruice TC. Comparison of the dynamics for ground-state and transition-state structures in the active site of catechol *O*-methyltransferase. J. Am. Chem. Soc 2000;122:7165–7171.
44. DeLano, WL. The PyMOL Molecular Graphics System. San Carlos, CA, USA: DeLano Scientific; 2002. http://www.pymol.org

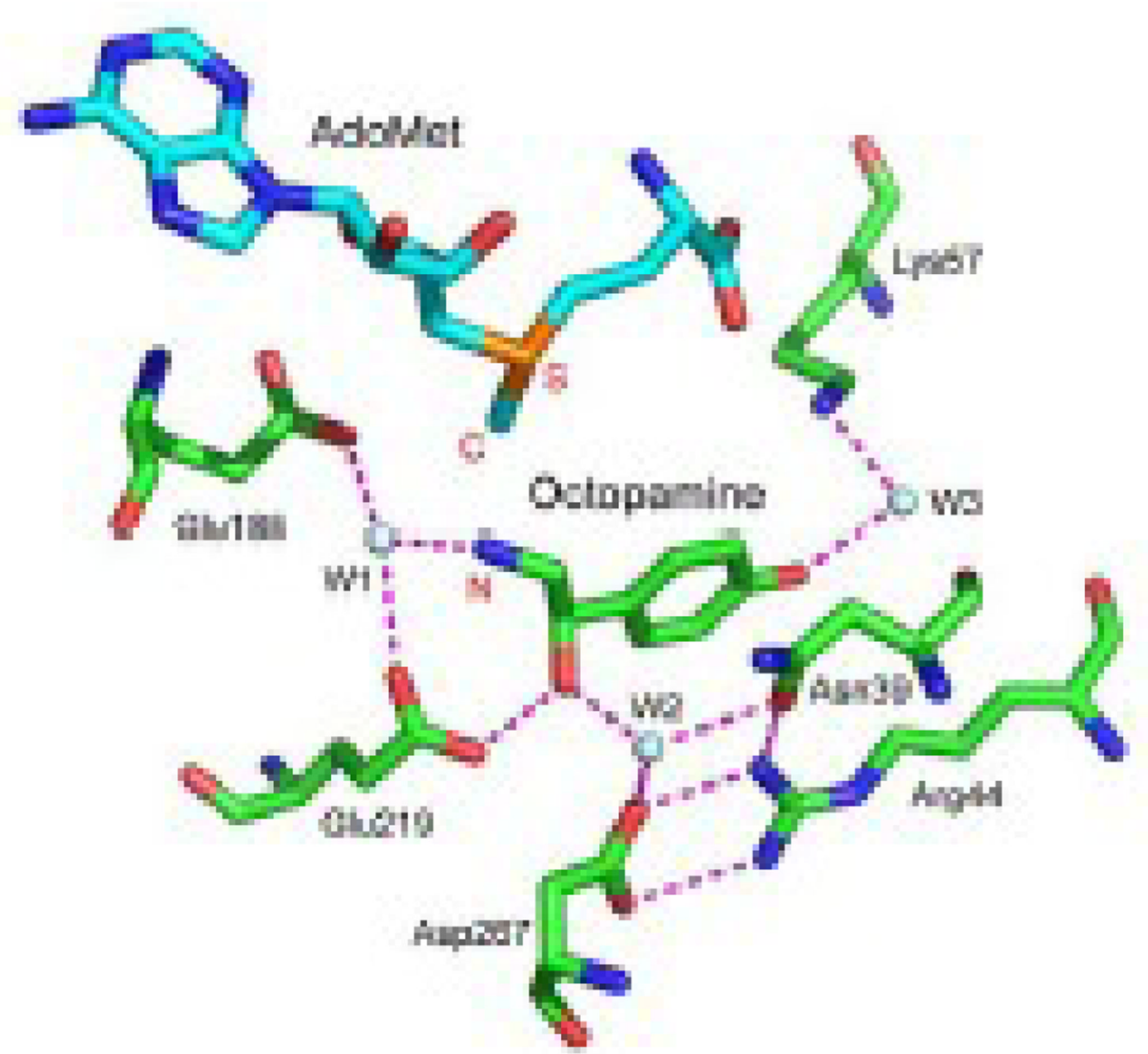

Figure 1.
Model structure of the active site of PNMT showing the two substrates, octopamine and AdoMet. Water molecules are in gray and the potential hydrogen bonding network is in magenta. As used in the text, N, C and S refer to the amine nitrogen, the methyl carbon, and the AdoMet sulfur, respectively. The AdoMet structure was from PDB 2G72 while octopamine and other active site residues were from PDB 2AN4. The figure was created using PyMol [44].

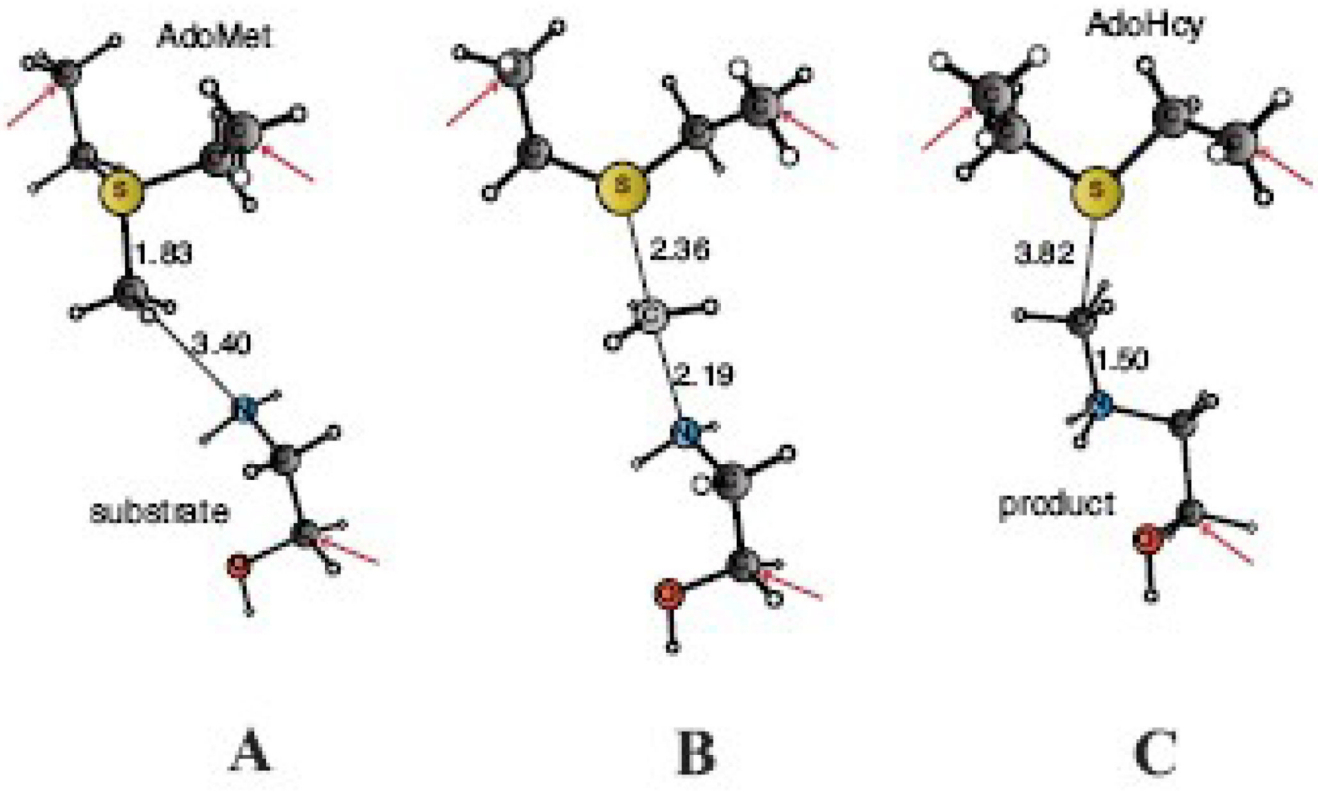

Figure 2.
Optimized reactant (A), methyl transfer transition state (B), and product (C) structures for Model A. Arrows indicate centers that are locked to their crystallographic positions during the geometry optimizations. Distances are given in angstrom.

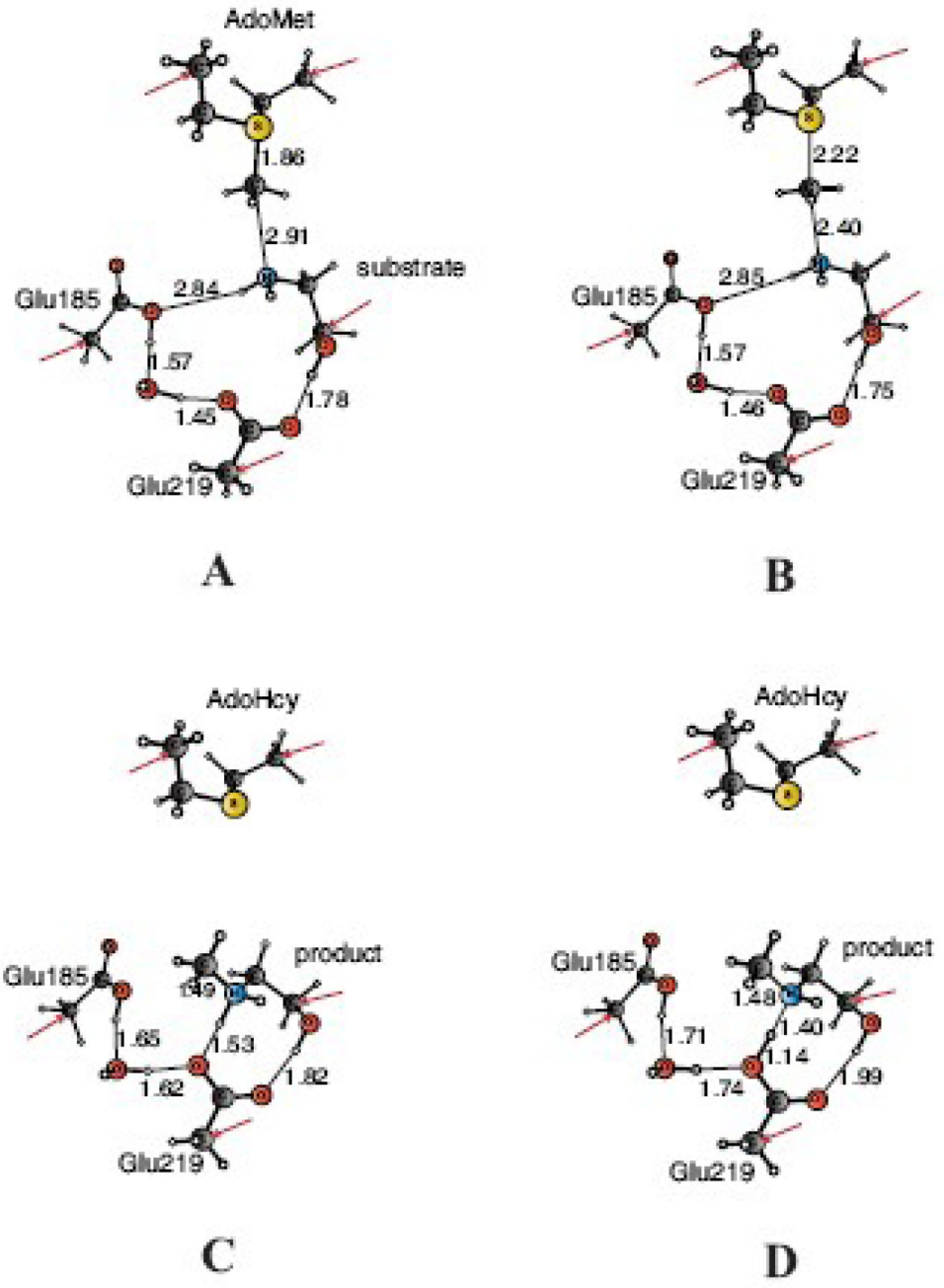

Figure 3.
Optimized reactant (A), methyl transfer transition state (B), and product structures (C and D) for Model B.

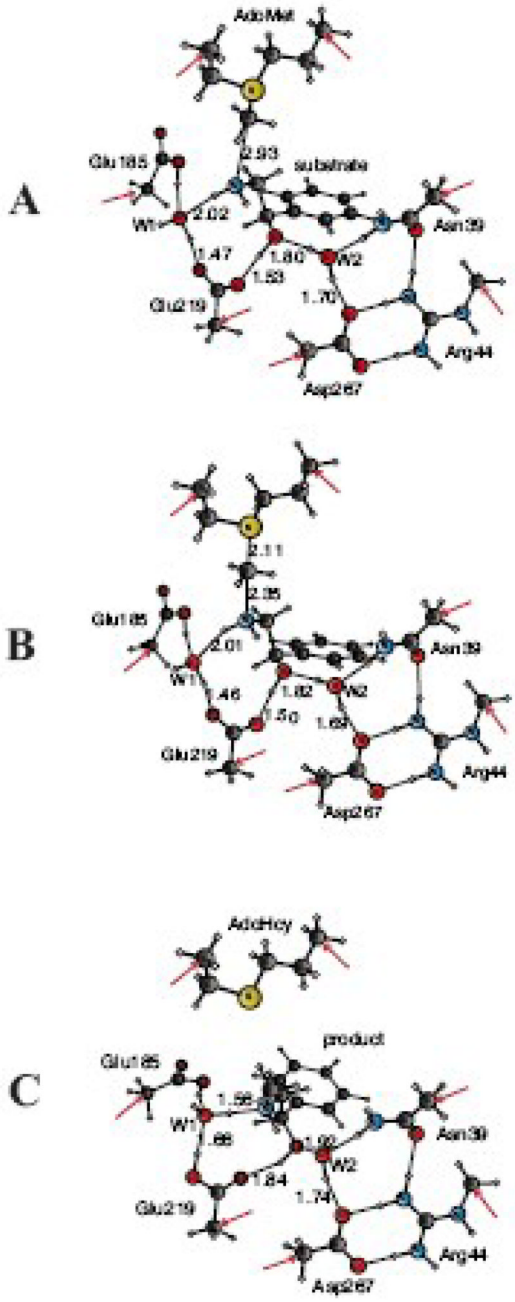

Figure 4.
Optimized structures of the reactant (A), transition state (B), and product (C) of Model C.

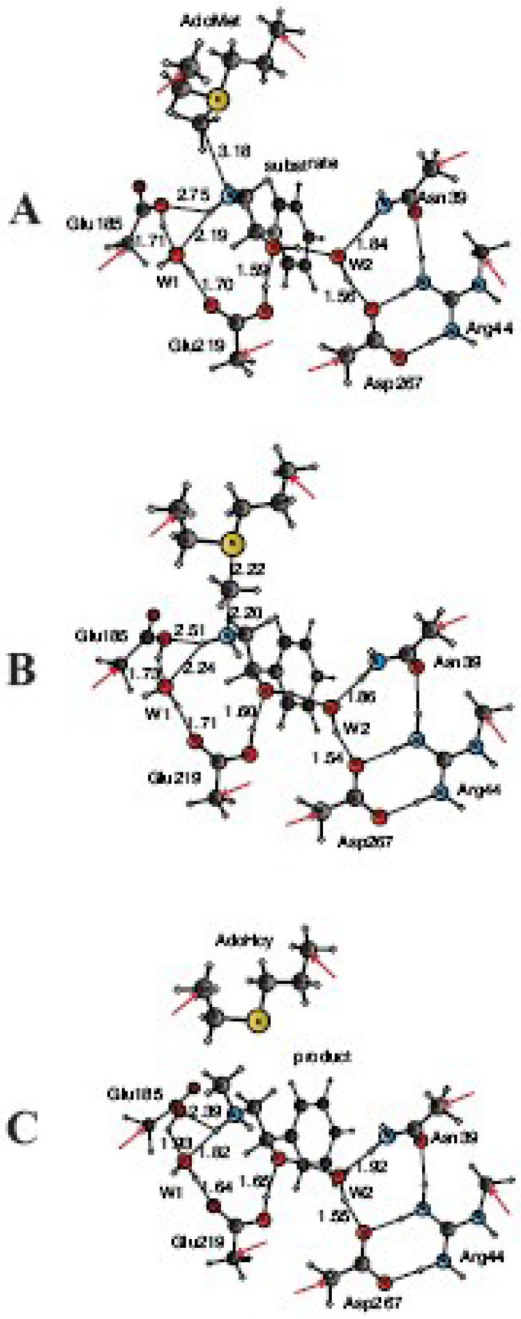

Figure 5.
Optimized reactant (A), transition state (B) and product (C) structures of Model C in the case of a protonated Glu219 residue, called Model C(H^+).

Table 1

Michaelis-Menten data for hPNMT variants[a].

hPNMT variant	K_n PEA (μM)	K_m AdoMet (μM)	k_{cat} (min^{-1})
Wildtype[b]	99 ± 6	3.4 ± 0.2	2.8 ± 0.1
E185A[b]	102 ± 6	1.7 ± 0.1	0.17 ± 0.01
E185Q[b]	101 ± 6	1.3 ± 0.1	0.01 ± 0.001
E219A[c]	580 ± 76	7.1 ± 0.8	1.3 ± 0.1
E219Q[b]	179 ± 17	6.7 ± 0.5	2.9 ± 0.1
E185A/E219A	124 ± 10	3.1 ± 0.3	0.29 ± 0.01

[a] Kinetic data were obtained in 50 mM phosphate buffer (pH 8.0) at 30 °C. Each data point is an average of at least three individual measurements. Values are reported as ± SEM (standard error of the mean).

[b] Data from Gee et al [15].

[c] Data from Wu et al. [32].

Table 2

Summary of the calculated barriers and reaction energies [kcal/mol] and important transition state distances [Å] for the various models.

	Barrier[a]			Reaction Energy			TS Distances	
	ε=1	ε=4	ε=80	ε=1	ε=4	ε=80	S–C	C–N
Model A	16.7	16.6	16.4	−5.7	−13.2	−15.8	2.36	2.19
Model B[b]	6.0	11.8	13.7	−48.3	−28.5	−21.8	2.22	2.40
				−47.9	−27.7	−20.9		
Model C	4.8	8.8	9.9	−47.9	−29.5	−28.3	2.11	2.35
Model C(H^+)	13.6	15.8	16.4	−18.1	−13.8	−12.5	2.22	2.20

[a] Experimental k_{cat} is 2.8 s^{-1}, which corresponds to an energy barrier of ~19 kcal/mol.

[b] Two product structures could be optimized for Model B, see text.